Materials Science and Engineering A xxx (2011) xxx–xxx

Contents lists available at SciVerse ScienceDirect

Materials Science and Engineering A

journal homepage: www.elsevier.com/locate/msea

Double-hit compression behavior of TWIP steels

J. Hajkazemi [a,*], A. Zarei-Hanzaki [a], M. Sabet [a], S. Khoddam [b]

[a] School of Metallurgy and Materials Engineering, University of Tehran, Tehran, Iran
[b] Department of Mechanical and Aerospace Engineering, Monash University, Clayton, VIC 3800, Australia

ARTICLE INFO

Article history:
Received 7 February 2011
Received in revised form 5 July 2011
Accepted 20 September 2011
Available online xxx

Keywords:
TWIP steels
Double-hit compression test
Static restoration
Static strain aging
Dislocation

ABSTRACT

The study of hot deformation characteristics of high-Mn twinning induced plasticity (TWIP) steels is of great importance due to their superior mechanical properties and potential applications for structural applications. In the present work, the static restoration behavior of 29 wt% Mn TWIP steel has been investigated using the double-hit compression testing technique. The tests were performed at 950–1150 °C under constant strain rate (0.1 s^{-1}). The results indicated a hardening behavior when the second pass deformation was applied after the interpass time. To justify the strengthening behavior different mechanisms were considered. The static strain aging phenomenon, involving interactions between interstitial atoms (carbon atoms) and dislocations were believed to be the main reasons of interpass hardening in this study. The retardation of restoration processes due to the formation of high frequency annealing twins during interpass time as planar obstacles to the dislocation glide were believed as other reasons to explain this phenomenon.

1. Introduction

In general to reduce the fuel consumption and the CO_2 emissions, the weight of vehicles should be reduced [1]. Subsequently the introduction of high strength materials with an excellent formability has been necessitated. This in turn has been followed by the development of new alloys in general and of steels in particular. Recently, a new class of high-Mn steels (15–30 wt% Mn) which are prone to the twinning induced plasticity effect has been developed [2,3]. The presence of fully austenitic microstructure in these steels is due to their low stacking fault energy (SFE) [4–6].

The main explanations for the excellent balance between flow stresses and ductility of TWIP steels are an atypical strain aging mechanism and the occurrence of deformation mechanisms additional to dislocation gliding [7–10]. Bake hardening (i.e., involving interactions between interstitial atoms and dislocations) is essentially a strain aging process and can be the main reason for increase in yield strength. Investigations on an ultra low carbon steel (with a total carbon content of 20 ppm) have established that the strengthening takes place in two stages: (a) a Cottrell atmosphere formation stage and (b) a precipitation stage. The yield stress first increase with aging time and reaches a maximum and then remains almost constant thereafter. Carbon segregation to the dislocations increases with increasing the applied pre-strain. As the dislocation density increases with the amount of applied pre-strain, the amount of carbon which contributes to Cottrell atmosphere formation on all the dislocations increases. Consequently, the amount of carbon contributing to the second stage of aging or precipitation decreases with higher pre-strain [8].

The microstructural evolution during recrystallization is highly dictated by the characteristics of the deformed matrix (including the stored energy content and the local chemistry), the orientation relationship between the deformed structure and the growing grain, the temperature, and so on. Therefore, twin boundaries may complicate the restoration processes in low SFE materials [11,12]. In fact, the twinned structure may change the energy and the mobility of a mobile interface, thereby either enhancing or retarding the evolution of a given microstructure [11–14].

To date the most research on high manganese TWIP steels has been conducted on their room temperature mechanical properties [1–6]. In the present work, the static restoration behavior of a grade of TWIP steels with 29 wt% manganese has been studied through utilizing the double-hit compression testing technique. In addition, the role of static strain aging mechanism and twin formation during the interpass time on the mechanical properties and microstructural evolution of the experimental TWIP steel has been investigated.

2. Experimental methods

The chemical composition of the experimental steel which was cast under an argon atmosphere is given in Table 1. In order to eliminate the undesired solidified structure and to achieve a fine

* Corresponding author at: School of Metallurgy and Materials Engineering, University of Tehran, Tehran, Iran. Tel.: +98 21 61114167; fax: +98 21 88006076.
E-mail address: jhajkazemi@ut.ac.ir (J. Hajkazemi).

0921-5093/$ – see front matter © 2011 Elsevier B.V. All rights reserved.
doi:10.1016/j.msea.2011.09.080

Table 1
The chemical composition of the experimental TWIP steel.

	C	Mn	Si	Al	P	S	Fe
wt%	0.013	29.10	0.30	2.40	0.06	0.06	Bal.

grain microstructure, the ingot was forged at 1150 °C. The forged material was annealed at 1100 °C for 45 min to chemically homogenize the microstructure. The material was then machined into the cylindrical specimens in accordance with the ASTM-F136 standard (12 mm in height and 8 mm in diameter).

The hot deformation tests were performed using an Instron-4208 universal testing machine equipped with a programmable furnace. Mica foil was inserted between the specimens and the compression anvils to reduce the friction. The specimens were heated to the test temperature, held for 300 s to homogenize the temperature and then compressed under a constant strain rate of 0.1 s^{-1} up to a predetermined strain. The amount of strain to be applied in each pass was estimated using the results of single-hit compression tests at the same strain rate [15]. The strain was determined in a way that the onset of dynamic recrystallization would be prevented. The double-hit compression tests were conducted at temperatures of 950, 1050 and 1150 °C with applying interpass times of 30, 80 and 300 s. To investigate the static restoration behavior of the experimental steel, a number of specimens were immediately water-quenched at the end of first pass, interpass time and second pass. This was followed by longitudinal sections and preparation for optical microscopy.

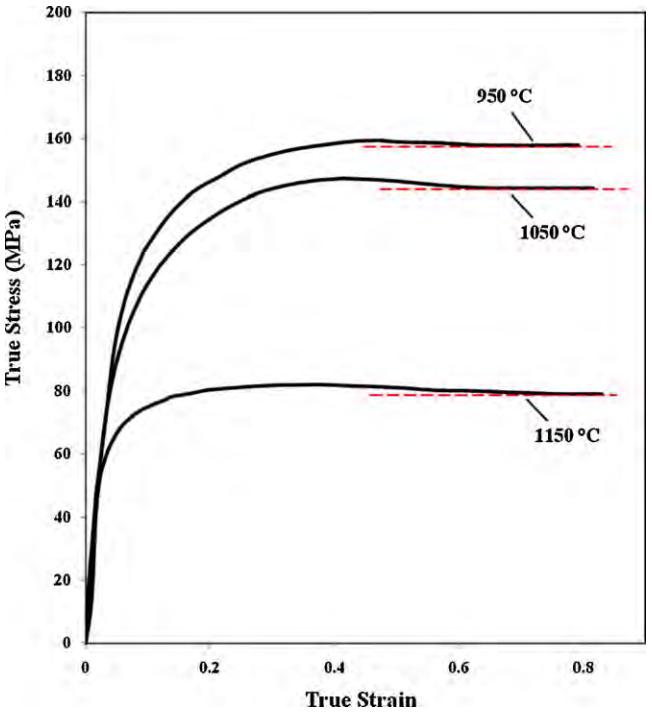

Fig. 2. The true stress–true strain curves of single-hit compression testing under strain rate of 0.1 s^{-1}.

3. Results and discussion

3.1. Initial microstructure

The optical microstructure of the solution annealed steel (1100 °C, 45 min, water quenched) is shown in Fig. 1. A fully austenitic microstructure characterized by annealing twins (shown by A.T. symbol in Fig. 1) is observed. The average initial grain size after solution annealing is 80 μm.

3.2. Critical strain for initiation of dynamic recrystallization (ε_C)

The typical true stress–true strain curves of single-hit compression tests are shown in Fig. 2. As is seen the flow stress decreases with increasing temperature (decreasing Zener–Hollomon parameter) at constant strain rate of 0.1 s^{-1}. In addition a single peak followed by a plateau is observed in all the curves. This is the main characteristic of discontinuous dynamic recrystallization (DRX) during hot deformation of metals and alloys [16]. Zarei-Hanzaki et al. in their previous studies on the microstructural evolution of the present material through single-hit compression testing under the same condition have confirmed the occurrence of DRX [15].

Dynamic recrystallization occurs where the applied strain (i.e., the accumulated dislocation density) reaches a critical value (ε_C) [16]. The latter is estimated from the true stress–the strain curves (Fig. 2) using the approach developed by Poliak and Jonas [17]. In this method, ε_C is associated with the point of inflection when the rate of hardening is plotted as a function of the flow stress (σ), (Fig. 3). The ε_C corresponding stress is the minimum in the curves in Fig. 3. As is seen σ_C decreases steadily with increasing temperature (decreasing Zener–Hollomon parameter). The results indicate that any pass of double-hit compression testing must be interrupted below a true strain of 0.2 (the amount of 0.17 was chosen in the present study).

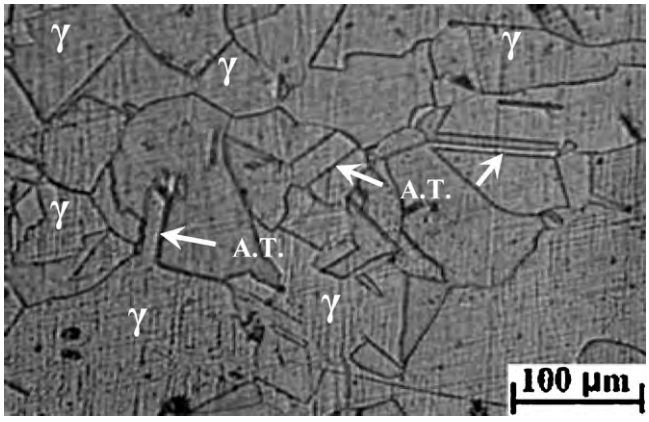

Fig. 1. Presence of annealing twins in the specimen annealed at 1100 °C for 45 min.

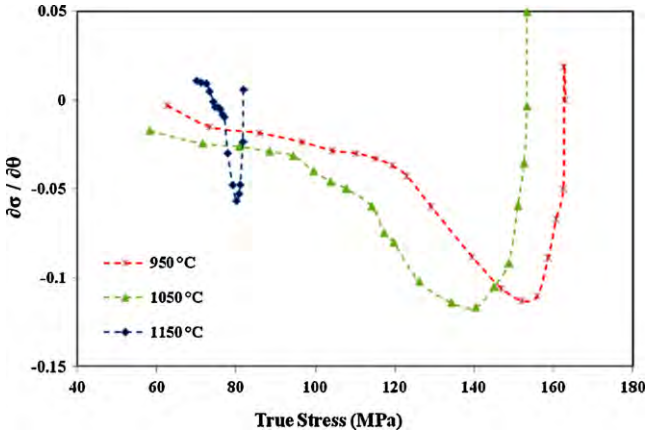

Fig. 3. The variation of hardening rate with flow stress at different temperatures; this has been utilized to estimate the ε_C and σ_C.

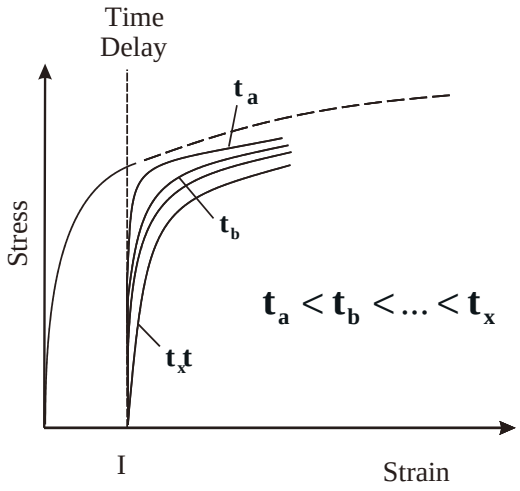

Fig. 4. A typical double hit flow stress with different interpass times.

3.3. Double-hit compression behavior

A typical schematics of the true stress–true strain flow curves of the double-hit compression tests is presented in Fig. 4 in which the interpass time dictates what percentage of the deformed material undergoes static recrystallization. Point I marks the beginning of the interruption between the two passes. A number of different interpass times ($t_a < t_b < \cdots < t_x$) have been chosen and their subsequent post deformation behavior have been overlaid in Fig. 4 for comparison [18].

Usually the time for 50% recrystallization can be empirically related to the strain rate, strain and temperature as [16]:

$$t_{50\%} = A\varepsilon^n \dot{\varepsilon}^m \exp\left(\frac{Q}{RT}\right) \quad (1)$$

in which A, n and m are the material constants. Q, R and T are activation energy, gas constant and temperature in Kelvin, respectively. $t_{50\%}$ is the time index which is used as a reference to describe the kinetics of static recrystallization according to the Avarami equation as:

$$X = 1 - \exp\left[-0.693\left(\frac{t}{t_{50\%}}\right)^{n'}\right] \quad (2)$$

in Eq. (2), t and n' are the holding time and Avrami index, respectively.

Fractional softening X has been used extensively in the literature to following the recrystallization behavior of austenite and this is be calculated as [18]:

$$X = \frac{\sigma_A - \sigma_E}{\sigma_A - \sigma_Y} \quad (3)$$

where σ_A, σ_E and σ_Y are the flow stress at the end of the first deformation, the yield stress of the second deformation and the yield stress of the first deformation, respectively.

The orthodox models described by Eqs. (1)–(3) indicate that after an interpass time t, the resultant static recrystallization reduces the hot strength.

Fig. 5 shows the unusual behavior of the TWIP samples during a double hit hot compression test which may be characterized by a strengthening phenomena taking place after an interpass time. One can observe that the yield stress has significantly increased in the second pass after the interpass time. In addition, the yield stress of the second pass reduces by increasing the interpass time at a constant temperature.

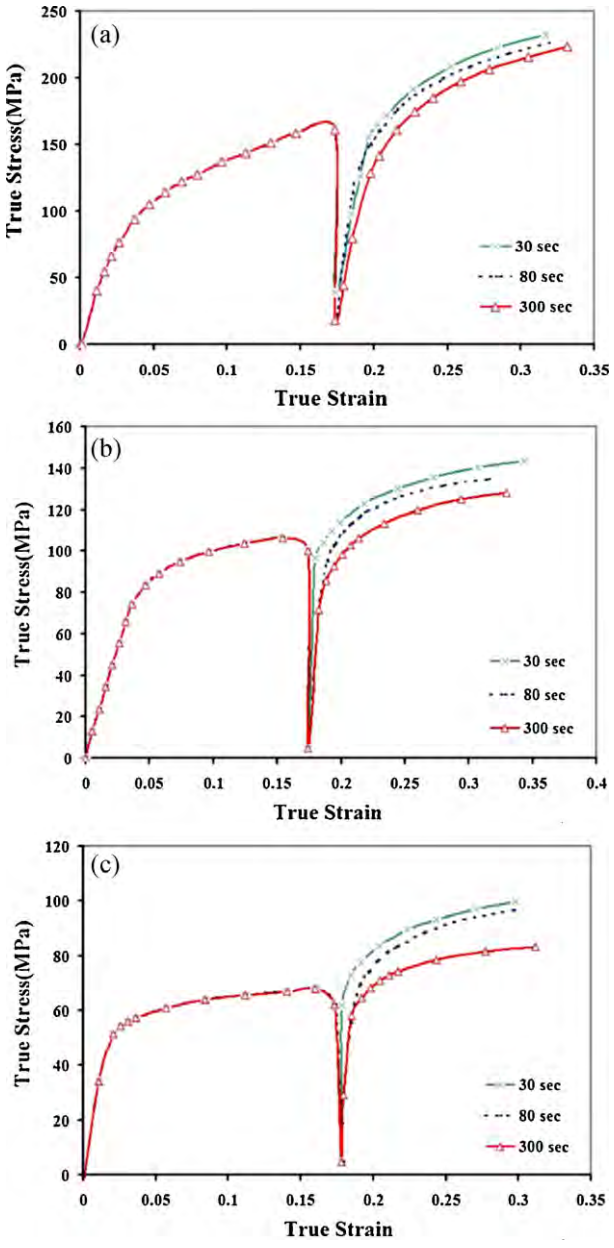

Fig. 5. The true stress–true strain curves of the experimental steel at strain rate of $0.1s^{-1}$ and (a) 950 °C, (b) 1050 °C and (c) 1150 °C.

The static recrystallization behavior is commonly examined using the fractional softening method [16]. Clearly, this method cannot be applied to the current material; no softening is observed. Instead, the progress of static recrystallization is thus inferred from the degree to which the yield stress increases after interpass time. The fractional hardening, X, is defined as:

$$X = \frac{\sigma_2 - \sigma_1}{\sigma_1} \quad (4)$$

where σ_1 and σ_2 are the respective yield stress of the first and second deformation step. The variations of the fractional hardening with interpass time at various temperatures are plotted in Fig. 6. As is seen, a similar strengthening trend is realized at all temperatures presented here.

Please cite this article in press as: J. Hajkazemi, et al., Mater. Sci. Eng. A (2011), doi:10.1016/j.msea.2011.09.080

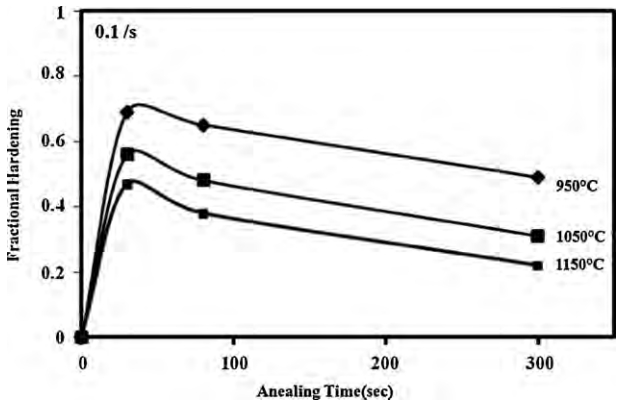

Fig. 6. The fractional hardening as a function of annealing time for various temperatures.

3.4. Microstructural evolution

The typical microstructures of the specimens after straining up to the true strain of 0.17 at various temperatures are shown in Fig. 7. The initial equiaxed grains that formed after homogenization were changed into pancaked ones. The latter contains the deformed incoherent twin boundaries. The area fraction of annealing twins before and after the first pass is equal and no annealing twins were formed during first pass. The deformed twins with incoherent boundaries (created during the first pass as the result of straining) are indicated by arrows in Fig. 7.

To investigate the effect of temperature and interpass time on microstructural evolution, the quenched microstructures of the experimental TWIP steel are considered in Fig. 8. These micrographs show that a rather high percentage of the structure has remained unrecrystallized at 950 °C. Upon holding at 950 °C for 80 s a few statically recrystallized grains were identified in the microstructure (depicted by white arrows in Fig. 8a). There is an increase in the size of new grains with elevating the temperature, after the same interpass time (Fig. 8c). As the grain growth involves the migration of high angle grain boundaries, its kinetics would be strongly influenced by the temperature. Consequently significant grain growth is often found at higher temperatures [16].

It is clearly seen in Fig. 8 that after holding the specimen for longer interpass time at 1150 °C, an extensive growth of new grains has occurred. As is well established, the static recrystallization is a nucleation and growth phenomena. Holding the specimen at the test temperature provides more time for growth and therefore a fully recrystallized structure containing large grains would be formed at the end of process. The microstructural observation also confirms this trend (Fig. 8b and c).

3.5. Interpass time strengthening

3.5.1. Static strain aging phenomenon

As is seen in Fig. 6, the yield stress after the relaxation time has been increased in all strain rates. In addition the steel has an outstanding lower yield stress in longer interpass times. The yield stress is thought to be the most representative parameter for dislocation motion and any object that restricts this motion can lead to enhance the stress level throughout the static strain aging mechanism. It is worth noting that this mechanism is consistent with a pinning mechanism related to the aging of dislocations, for example, due to the diffusion of carbon atoms. Since the carbon mobility is rather low in TWIP steels, alternative aging mechanisms involving, for example, rotation of atom–vacancy complexes have also been discussed in the literature (e.g. [8]). Besides, it is known that high temperature deformation leads to intensify the diffusivity of C atoms and therefore the expansion of pinned dislocations.

Given the wide range of SFE of the above materials, the effect of C is most likely due to its direct interaction with dislocations as opposed to its indirect effect through the increase in SFE [10]. It is known that during strain aging, the first carbon atoms which reach the dislocations anchor them more strongly than those arriving at a later stage of the atmosphere formation [12]. In longer relaxation time, extension of recrystallized structure leads to decrease the hardening rate at the beginning the second pass deformation (Fig. 6).

3.5.2. Annealing twins effect

The area fraction of annealing twins in each microstructure was analyzed quantitatively by image software tools. The frequency of twins has extremely increased after the interpass time. For instance, some annealing twins with high angle boundaries have been accommodated inside the new grains (shown with arrows in Fig. 8c). In fact, the recrystallized grains appear to be partitioned into smaller regions by the aforementioned annealing twins. Furthermore the increase of temperature and interpass time led to lower twin frequency. This may be related to the occurrence of extensive SRX and therefore the annihilation of deformed structure. However, as is well established the annealing twins would form during restoration processes [11,19–23]. The twin formation may continue up to the later stage of the grain growth thereby enhancing the high angle boundaries area in the microstructure [23,24]. It has often been observed that during recrystallization where the grain growth becomes stagnant, annealing twins would form to resume the growth. In fact in these cases the boundaries between the recrystallized grain and the deformed matrix are often in a region of low dislocation density and/or low misorientation angle. Twinning alters the misorientation and apparently offer the additional boundary energy required to continue the growth [19].

A precise study on the microstructures has indicated that two groups of twins can be distinguished after the relaxation time, Fig. 9. The first one is primary twins (PT) which were initially present in the microstructure before applying the first hit and lost their coherency after straining (indicated by PT in Fig. 9). In addition to these incoherence twins, there are a group of twins with fully coherent and straight boundaries. This second group of twins formed during the interpass time (these are indicated by ST in Fig. 9). In fact, as has been recently clarified the low SFE is believed to be the main reason for the relatively wide range of twin formation [11,19,23]. Due to the low SFE of these steels, many stacking fault regions form in the microstructure during deformation. This is considered as a high driving force for the formation of secondary twins. In fact the SFs are one of the preferred regions for annealing twin formation [24,25], and by this the experimented steel is extremely prone to form annealing twins after interpass time.

The secondary twins can have an important role in enhancing the strength [21,25]. Nevertheless the twin's frequency has been lowered by increasing the temperature and interpass time. It is worth noting that the aforementioned interpass time strengthening behavior exactly follows the trend of twin's frequency changes. As is well established the twin boundaries play a major role in the strain-hardening response of low SFE metals and alloys [26–28]. The contribution of twinning to the strain hardening is derived largely from the fact that the twin boundaries act as active barriers for dislocation pile-ups and storage (similar to grain boundaries). The latter comes from the fact that the slip lengths are significantly reduced by twin formation thereby promoting dislocation accumulation and storage. Several analytical [29,30] and experimental studies [31,28] support this notion. The previous attempts to model the influence of twinning on work hardening of metallic alloys were combined with modeling the influence of grain size on the rate

Please cite this article in press as: J. Hajkazemi, et al., Mater. Sci. Eng. A (2011), doi:10.1016/j.msea.2011.09.080

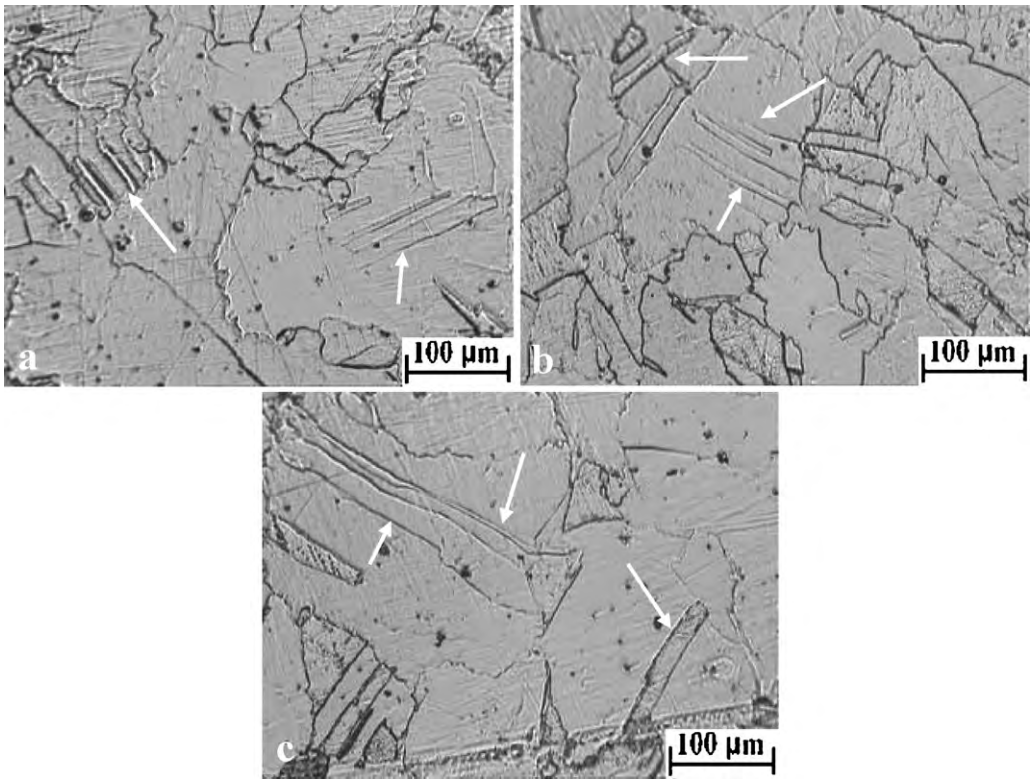

Fig. 7. The microstructures of the experimental steel right after applying the first deformation pass under strain rate of 10^{-1} s^{-1} and at temperatures of (a) 950 °C, (b) 1050 °C and (c) 1150 °C.

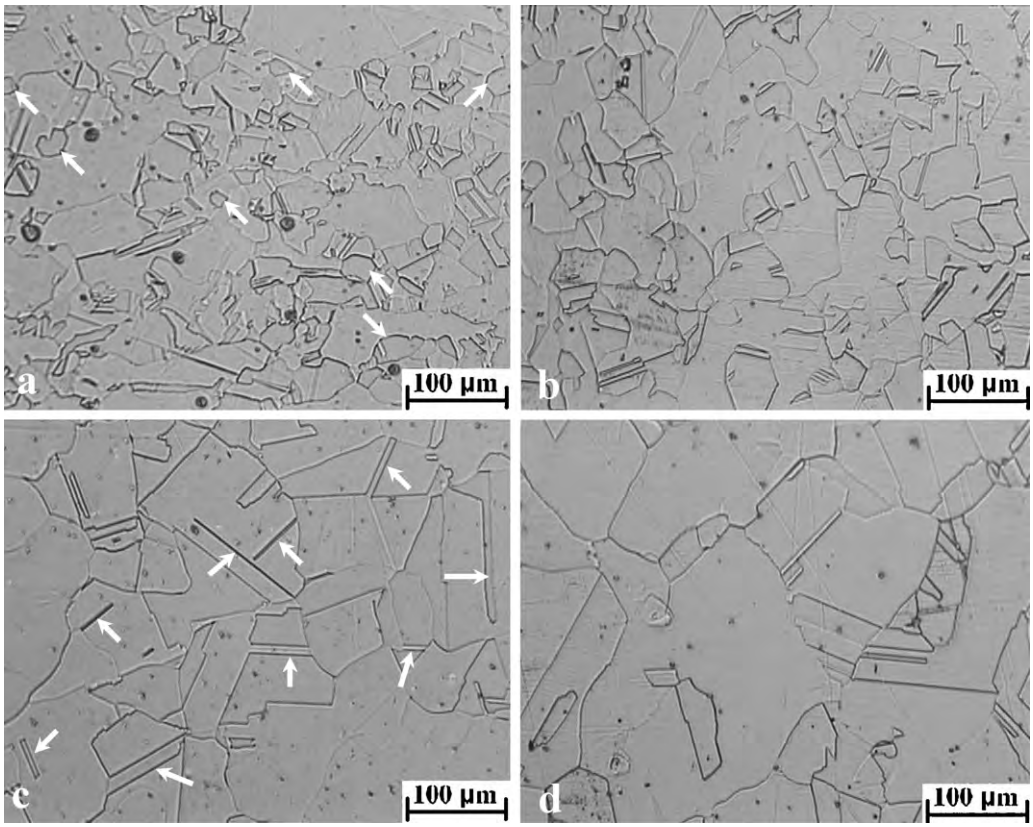

Fig. 8. The typical microstructures of the experimental steel interrupted and quenched after: (a) 80 s interpass time at 950 °C, (b) 30 s interpass time at 1150 °C, (c) 80 s interpass time at 1150 °C and (d) 300 s interpass time at 1150 °C.

Please cite this article in press as: J. Hajkazemi, et al., Mater. Sci. Eng. A (2011), doi:10.1016/j.msea.2011.09.080

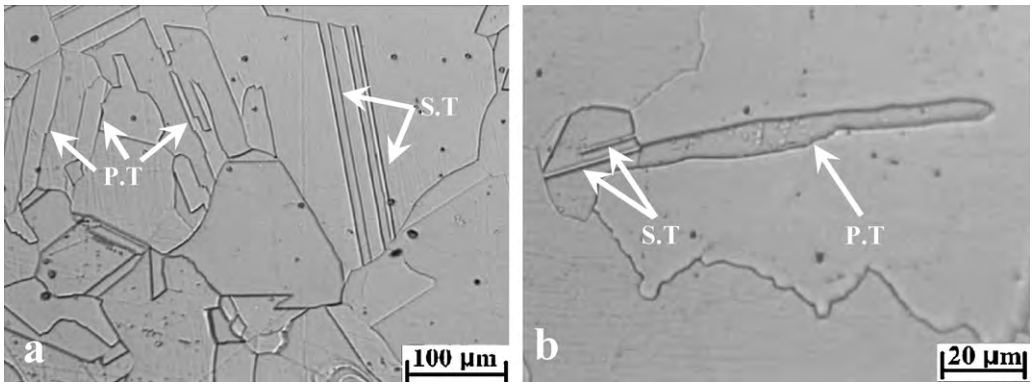

Fig. 9. The optical microstructure of the specimens deformed under 10^{-1} s^{-1} up to strain of 0.2: (a) after interpass time of 300 s at 1150 °C and (b) after interpass time of 80 s at 1050 °C.

of strengthening. These models are extensions of the Hall–Petch relationship [19].

Another significant factor that should be considered is the state of twin boundaries. The primary twins hold the full coherent boundaries before applying the first pass. These changes to incoherent ones after applying the first pass. Some of these incoherent boundaries are eliminated via recrystallization during interpass time and the rest remains unchanged until starting the second pass. The effect of these boundaries on impeding the dislocations slip and strengthening is more than that of coherent boundaries. Therefore, the presence of primary twins with incoherent boundaries is another strengthening factor in the present study.

4. Conclusions

In the present study, the double-hit compression behavior of TWIP steels in the temperature range of 950–1150 °C and under strain rate of 0.1 s^{-1} has been investigated and the following conclusions have been drawn:

1. After holding the TWIP steel for different interpass times, the yield stress of the second pass has been unexpectedly elevated in comparison to the first pass.
2. It is suggested that static strain aging can play an important role in the hardening behavior observed after relaxation time.
3. The fractional hardening level is dropped as the relaxation time increased. In fact longer aging time leads to higher volume fraction of recrystallized structure and decrease the hardening at the beginning of the second pass deformation.
4. The twin formation during interpass time is another reason for interpass strengthening of TWIP steels. The contribution of twinning to the strain hardening is derived largely from the fact that the twin boundaries act as active barriers for dislocation pile-ups and storage (similar to grain boundaries).
5. The primary twins which have lost their coherency due to the straining are considered as the second main reason for interpass time strengthening phenomena.

References

[1] A.S. Hamada, L.P. Karjalainen, Mater. Sci. Eng. A 467 (2007) 114–124.
[2] Georg Frommeyer, Udo Brux, ISIJ Int. 43 (2003) 438–446.
[3] B. Qin, H.K.D.H. Bhadeshia, Mater. Sci. Technol. 24 (2008) 969–973.
[4] B.X. Huang, X.D. Wang, Mater. Sci. Eng. A 438–440 (2006) 306–311.
[5] M. Iker, D. Gaude-Fugarolas, Adv. Mater. Res. 15–17 (2007) 852–857.
[6] S. Vercammen, B. Blanpain, Acta Mater. 52 (2004) 2005–2012.
[7] S. Allain, O. Bouaziz, T. Lebedkina, Scripta Mater. 64 (2011) 741–744.
[8] J.A.K. Dea, K. De Blauweb, S. Vandeputteb, B.C. De Coomana, J. Alloys Compd. 310 (2000) 405–410.
[9] S. Allain, O. Bouaziza, J.P. Chateau, Scripta Mater. 62 (2010) 500–503.
[10] X. Wang, H.S. Zurob, J.D. Embury, X. Ren, Mater. Sci. Eng. A 527 (2010) 3785–3791.
[11] A.R. Jones, J. Mater. Sci. 16 (1981) 1374–1380.
[12] O. Bouaziz, S. Allain, Scripta Mater. 58 (2008) 484–487.
[13] X. Wang, E. Brunger, G. Gottstein, Scripta Mater. 46 (2002) 875–880.
[14] Mukul Kumar, J. Adam, Schwartz, Acta Mater. 50 (2002) 2599–2612.
[15] M. Sabet, A. Zarei-Hanzaki, Sh. Khoddam, J. Eng. Mater. Technol. 131 (2009) 044502–44511.
[16] F.J. Humphreys, M. Hatherly, Recrystallization and Related Annealing Phenomena, Pergamon, Oxford, UK, 2003.
[17] G. Gottstein, M. Frommert, M. Goerdeler, Mater. Sci. Eng. A 387–389 (2004) 604–608.
[18] H.L. Andrade, M.G. Akben, J.J. Jonas, Metall. Trans. A 14A (1983) 1967–1977.
[19] D.P. Field, L.T. Bradford, Acta Mater. 55 (2007) 4233–4241.
[20] Y. Wang, Mater. Sci. Eng. A 497 (2008) 479–486.
[21] A. Clarissa, Yablinsky, K. Ellen, A. Cerreta, Metall. Mater. Trans. A 37 (2006) 1907–1914.
[22] O. Bouaziz, N. Guelton, Mater. Sci. Eng. A 319–321 (2001) 246–249.
[23] M.M. Myshlyaev, H.J. McQueen, Mater. Sci. Eng. A 337 (2002) 121–133.
[24] B.B. Rath, M.A. Imam, Mater. Phys. Mech. 1 (2000) 61–66.
[25] T. Baudin, A.L. Etter, R. Penelle, Mater. Charact. 58 (2007) 947–952.
[26] Mullner, C. Solenthaler, M.O. Speidel, Acta Metall. Mater. 42 (1994) 1727–1732.
[27] J. Christian, S. Mahajan, Mater. Sci. 39 (1995) 1–157.
[28] S. Asgari, E. El-danaf, R.D. Kalidindi, Metall. Trans. A 28 (1997) 1781–1789.
[29] S. Mahajan, Acta Metall. 21 (1973) 173–178.
[30] L. Remy, Acta Metall. 25 (1977) 711–717.
[31] L. Remy, Acta Metall. 26 (1978) 443–451.

Please cite this article in press as: J. Hajkazemi, et al., Mater. Sci. Eng. A (2011), doi:10.1016/j.msea.2011.09.080